SDSS'Rio 2010 STABILITY AND DUCTILITY OF STEEL STRUCTURES
E. Batista, P. Vellasco, L. de Lima (Eds.)
Rio de Janeiro, Brazil, September 8 - 10, 2010

INVESTIGATION OF THE TEST METHOD FOR DISTORTIONAL BUCKLING OF COMPRESSED PALLET RACK MEMBERS

Miquel Casafont*, Magdalena Pastor*, Francesc Roure* and Teoman Peköz**

* E.T.S. d'Enginyeria Industrial de Barcelona, Universitat Politècnica de Catalunya, Av. Diagonal 647, 08028, Barcelona, Spain.
e-mails: miquel.casafont@upc.edu, m.magdalena.pastor@upc.edu, francesc.roure@upc.edu

** School of Civil & Environmental Engineering, Cornell University, Ithaca, N Y 14853, USA
e-mail: tp26@cornell.edu

Keywords: Distortional buckling, rack structures, experimental tests, Generalized Beam Theory.

Abstract. *An investigation of the test methods for distortional buckling of perforated pallet rack members subjected to compression is presented. One of the key points of this test is the length of the specimen. According to the AISI Test Standard S910-08, the specimen length should be sufficiently short to minimize overall column effects, and sufficiently long to minimize end effects during loading. The aim of the investigation is to set a procedure for determining the specimen length according to this condition. Four different pallet rack sections are analysed and tested. Testing lengths are chosen from results of finite element linear buckling analyses and Direct Strength Method calculations. Distortional buckling was expected to be the dominant failure mode for some of the specimens tested. However, in the end, all experimental failures showed a significant participation of global buckling modes. The paper presents a discussion on the specimen behaviour observed in the tests, and some considerations concerning the effect of end support conditions on the experimental results.*

1 INTRODUCTION

Uprights of pallet rack structures contain a large amount of holes uniformly distributed along their length. These holes make easy the connection between the uprights and the other members of the rack structure. However, from the design point of view, the presence of the holes is a problem. Although many investigations of the effect of perforations on the strength of members have been performed, a definitive solution for pallet rack members has not yet been found. As a consequence, current standards recommend determining the load carrying capacity of uprights from experimental tests [1], [2].

This paper presents part of an investigation focused on the compression test that should be performed to determine the distortional buckling strength of uprights. The two main goals of the whole research work are: to check the effect of different end supports on the results of tests; and to determine the length of the specimens to capture the distortional buckling mode. Two different end boundary conditions will be investigated: the first one is pinned with respect to the global flexural modes of buckling, and fixed with respect to the torsional mode (as it is prescribed in the European standards [1]); while in the second one, all global modes are fixed (as it is prescribed in the American standards [2],[3]). However, at the moment of writing the present paper, only experimental results on the second type of end connection are available. For this reason, only fixed end supports (globally fixed end supports) are considered herein. In both tests setups, the end supports are fixed with respect to the distortional buckling mode (locally fixed), since warping of the end cross section is fully restrained. Actually, it is difficult in practice to carry out compression tests with locally pinned end supports.

It should be noticed that in an actual upright frame (see figure 1), the supports of the compressed members are neither fixed nor pinned with respect to the global modes and, most important, they are not locally fixed. For this reason, tests should be performed in such a way that the fixed distortional end conditions do not significantly increase the experimental ultimate load. This can be achieved by carrying out tests on long members, where several distortional half-sine waves can develop (see [4]). However, at the same time, very long members should also be avoided because the participation of distortional buckling in the failure mode becomes smaller as the member length increases. The problem can be summarized as follows: "the specimen length should be sufficiently short to minimize overall column effects, and sufficiently long to minimize end effects during loading" (AISI test Standard S910-08 [3]).

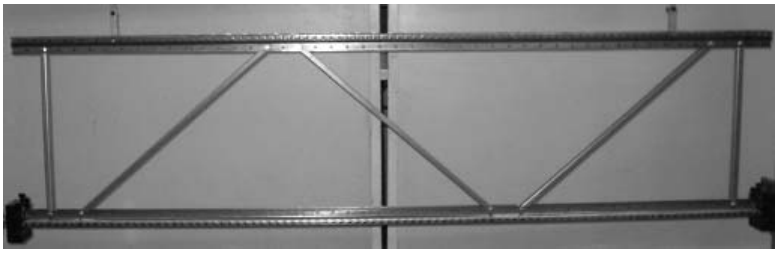

Figure 1: Pallet rack frame.

The part of the investigation presented in this paper is mainly focused on finding a way to determine the length of the specimens to be tested. Four different pallet rack cross-sections of medium load carrying capacity are chosen for analysis and testing (see figure 2). Tests are carried out on members of different lengths, expecting that the distortional mode of failure will be captured in such a way that the above mentioned condition is accomplished. The first step of the investigation was to choose the lengths of the specimens. These lengths were set on the basis of results of linear buckling analyses performed via the Finite Element Method. Afterwards, approximate Direct Strength Method calculations, carried out taking into account the effect of perforations, were performed to verify that distortional buckling failures would occur for the member lengths chosen. The results of these analyses and calculations are explained in the second section of the paper. Afterwards, compression tests were performed on the four cross-sections. The test setup and the experimental results are shown in Section 3. Sections 4 and 5 present a discussion on the specimen behavior observed in the tests. The deformation of the members, which was measured during loading, is analyzed. The investigation is still in progress, but some conclusions can be drawn from the work carried out until now. These conclusions are included in Section 6.

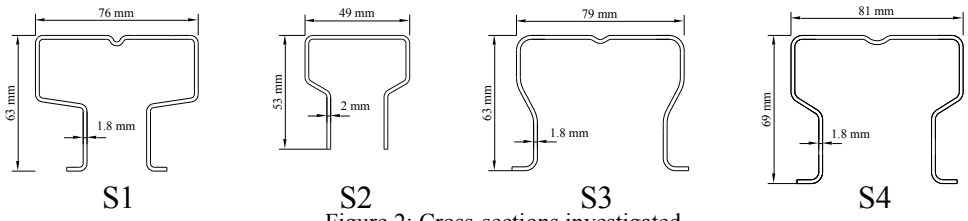

Figure 2: Cross-sections investigated.

2 SPECIMEN LENGTH

The specimen length will be expressed in terms of the critical distortional length, L_{crD}, that can easily be calculated via the Finite Strip Method (CUFSM [5]) or the Generalized Beam Theory (GBTUL [6]). Figure 3a shows the result of the linear buckling analysis carried out to cross-section S4 by means of the

CUFSM program. The critical length is highlighted with an arrow. In the present investigation, L_{crD} is the length of the minimum elastic distortional stress of a simply supported member.

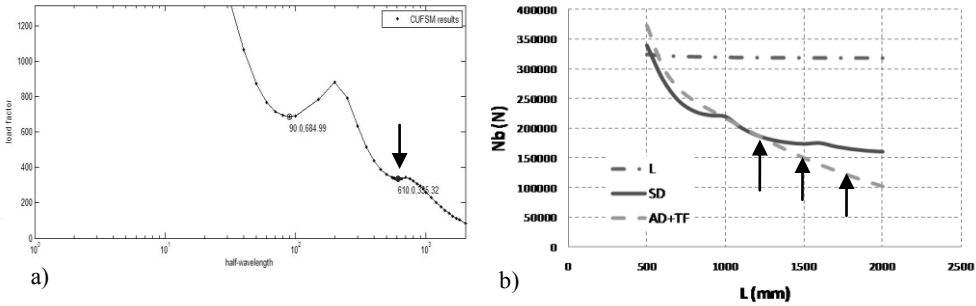

Figure 3: Results of linear buckling analyses of S4: a) CUFSM; b) FEM.

The CUFSM linear buckling analyses were carried out two times: first without considering the effect of perforations, modeling the gross cross-section of the member (L_{crD} in table 1); and second taking into account the holes by means of an equivalent thickness of the perforated web of the cross-section (L_{crDp} in table 1) (see [7]):

$$t_e = \left[\frac{L_p}{L} \cdot \frac{b_{wnp}}{b_w} + \left(1 - \frac{L_p}{L} \right) \right] \cdot t \,, \tag{1}$$

where: L_p is the length of the perforated part of the member; L is the length of the member; b_w is the web width; and b_{wnp} is the non-perforated part of the web. Alternative approaches to determining the effects of perforations are being studied by the authors at the present time.

Table 1: Results of the preliminary calculations.

L_{crD}: critical distortional length calculated with t; L_{crDp}: critical distortional length calculated with t_e; L_{ti}: specimen length expressed in terms of L_{crDp}; First G: minimum length for critical/failure mode.

Cross-section	L_{crD} (mm)	L_{crDp} (mm)	L_{t1} ($\cdot L_{crDp}$)	L_{t2} ($\cdot L_{crDp}$)	L_{t3} ($\cdot L_{crDp}$)	First G FEM ($\cdot L_{crDp}$)	First G DSM ($\cdot L_{crDp}$)
S1	570	630	2.06	2.61	3.09	2.06	2.61
S2	230	270	2.77	3.24	3.70	3.70	3.24
S3	420	450	2.00	2.46	-	2.46	>2.46
S4	520	610	1.96	2.45	2.95	1.96	2.95

Afterwards, linear buckling finite element analyses of the members were carried out. Perforations were included in the model together with the test boundary conditions (fixed ends). Figure 3b shows the result of the analysis performed to cross-section S4. The arrows point to the member lengths chosen for the tests (see table 1 for the other cross-sections). The idea is to test at the end of the interval where the symmetric-distortional mode is critical. Members as long as possible are tested to minimize the effects of end supports. This is the reason why the lowest specimen length was limited to $2 \cdot L_{crDp}$. (Note that the critical mode of cross-sections S1 and S4 for this length is not SD. This length is just at the beginning of their global interval.)

The next step was to apply the Direct Strength Method (DSM) to the four cross-sections. Column FIRST G DSM of table 1 shows the first length whose DSM predicted failure mode is global. It can be observed that the specimen lengths chosen are at the end of the length interval where distortional mode is

dominant, and at the beginning of the global mode interval. The DSM calculations were performed applying the equivalent thickness t_e (1).

3 TEST SETUP AND EXPERIMENTAL RESULTS

The first step of the experimental campaign was to carry out tensile coupon tests to determine the material properties of the steel of each profile. Afterwards, two sets of compression tests on uprights were performed. In the first set, all four sections of figure 2 were tested, while in the second one tests were only carried out on sections S1 and S4. The test setup of the first series is slightly simpler than in the second one. At each end of the specimen loading plates with special grips are fixed to the upright, so that the in plane deformation of the end cross-sections is locally restrained (see figure 4a). The specimens are placed horizontally in the rectangular frame shown in figure 4b. The loading plate of one end is directly bolted to the frame and, consequently, has all its degrees of freedom restrained. The loading plate of the other end is bolted to a 200 kN hydraulic jack, and has all its degrees of freedom restrained, except the axial displacement. Both ends are considered locally and globally fixed. The test is load controlled and the loading rate applied is 150 N/s.

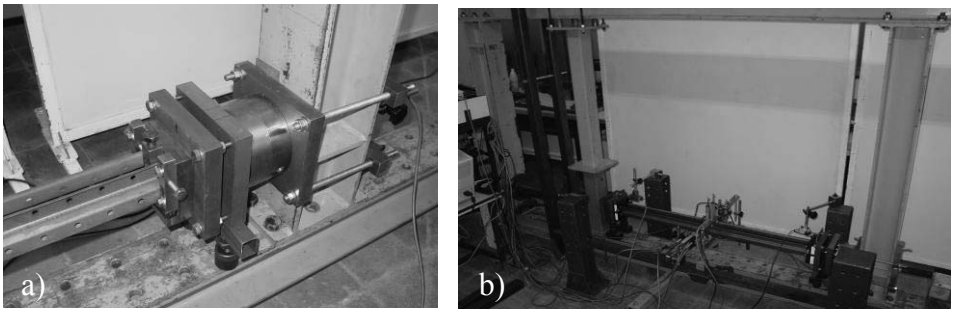

Figure 4: Test setup: a) Specimen end support with grip; b) Testing frame.

In this first set of tests only the applied load was measured by means of a load cell. Table 2 shows the ultimate loads and the failure modes of the specimens observed at the end of each test.

In the second set of compression tests, displacement transducers were placed at the end plates to measure the shortening of the specimen, and at the midpoint of the member to measure the cross-section deformation (figure 4b). Furthermore, tests were performed with two different types of loading plates: plates with special grips, such as those shown in figure 4a; and plates welded to the end cross-sections of the member. The idea was to check if similar results are obtained with both end plates. Another improvement was introduced to the test setup: the load plates are initially pinned (with a steel ball placed at the effective centre of gravity of the cross-section), a pre-compression is applied, and the end plates are allowed to self-align and compensate the specimen perpendicularity errors. Then the plates are blocked in this position with four bolts (figure 4a). Finally the compression test can be started. This type of fixed-adjustable plate device has the advantage that no precise machining of the ends of the upright are needed. Table 3 shows the results of the second set of tests.

4 DEFORMATION OF THE CENTRAL CROSS-SECTION

During the first set of tests, it was observed that in some specimens the final failure seemed to be a combination of distortional and global buckling modes. Mainly anti-symmetric distortional mode (AD) combined with torsional flexural buckling mode (TF). This combination was already observed when

Table 2: Experimental results of the first set of tests.
SD: symmetric distortional mode; AD: anti-symmetrical distortional mode; TF: torsional flexural mode.

Cross-section	L_{ti}/L_{crDp}	1st specimen		2nd specimen		3rd specimen	
		N_u (N)	Mode of failure	N_u (N)	Mode of failure	N_u (N)	Mode of failure
S1	2.06	126509	AD+TF	122095	AD+TF	123458	SD-->TF
	2.61	125303	TF	118887	TF	120358	TF
	3.09	94401	TF	92351	TF	94764	TF
S2	2.77	65501	SD+TF	71014	SD+TF	65108	AD+TF
	3.24	57417	(AD+) TF	58153	AD +TF	73761	AD+TF
	3.70	54190	(AD+) TF	52548	TF	60076	TF
S3	2	94548	AD (+TF)	85778	AD (+TF)	92243	SD (+TF)
	2.46	77204	(AD+) TF	92881	(AD+) TF	93116	AD+TF
S4	1.96	130051	(AD+) TF	104535	AD+TF	105016	AD (+TF)
	2.45	96638	(AD+) TF	102475	TF	117502	(AD+) TF
	2.95	84591	TF	86053	TF	85386	TF

Table 3: Experimental results of the second set of tests.
SD: symmetric distortional mode; AD: anti-symmetrical distortional mode; TF: torsional flexural mode.

Cross-section	L_{ti}/L_{crDp}	1st specimen		2nd specimen		3rd specimen	
		N_u (N)	Mode of failure	N_u (N)	Mode of failure	N_u (N)	Mode of failure
S1 Grips	2.06	139490	TF	135578	(AD+) TF	131618	(AD+) TF
S1 Welded	2.06	131595	TF	133930	(AD+) TF	134607	AD+TF
	2.61	123598	TF	112055	TF	117895	TF
S4 Grips	1.96	110912	(AD+) TF	114243	AD+TF	116811	AD+TF
S4 Welded	1.96	108219	AD (+TF)	108046	AD (+TF)	114606	SD
	2.45	98977	AD+TF	102887	AD+TF	-	-

carrying out the FEM linear buckling analysis. For instance, in figure 3b the critical buckling mode of the 1200 mm long S4 member is not a pure TF mode, it is a combination of AD+TF modes.

In view of these results, it was decided to use displacement transducers to measure the deformation of the central cross-section of the member. The goal was to know in which degree the distortional mode is combined with the global TF buckling mode. The transducers also provide with information about the deformation of the cross-section all along the loading process, which cannot be perceived by visual observation of the specimen.

From the displacements measured with the eight transducers, the four rotations shown in figure 5 were calculated and graphed. WR1 and WR2 are called web rotations, and FR1 and FR2 flange rotations. Figure 6 shows four graphs of rotations measured during loading, until ultimate load. The first three correspond to members whose length is about 2 times L_{crDp}, and the last one correspond to a $2.61 \cdot L_{crDp}$ member. In the first one (figure 6a), progressive opening of the flanges during loading can be seen, like in a symmetric deformational mode. However, at the end of the test the failure is of torsional type (TF), since all rotations went to the same side. The second one (figure 6b) is anti-symmetric (AD), and the final

failure also shows torsion. The third graph (figure 6c) is the most commonly observed behavior. It is similar to the first graph, but with a significant participation of torsion from the beginning. Finally, the last graph (figure 6d) is analogous to the second one, but in this case flange and web rotations are of the same magnitude. This indicates that the participation of distortional deformations is low.

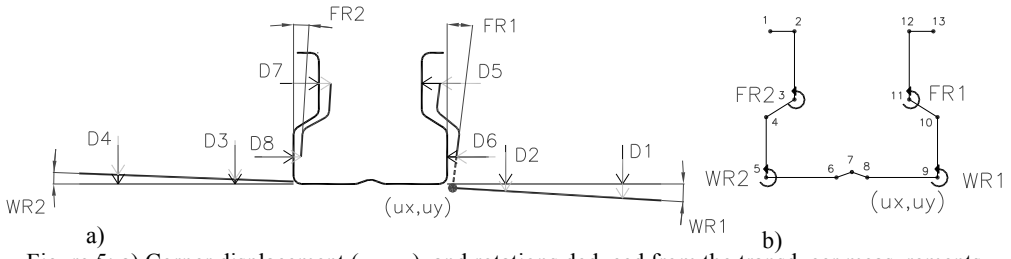

Figure 5: a) Corner displacement (ux,uy), and rotations deduced from the transducer measurements. b)Beam model of the cross-section.

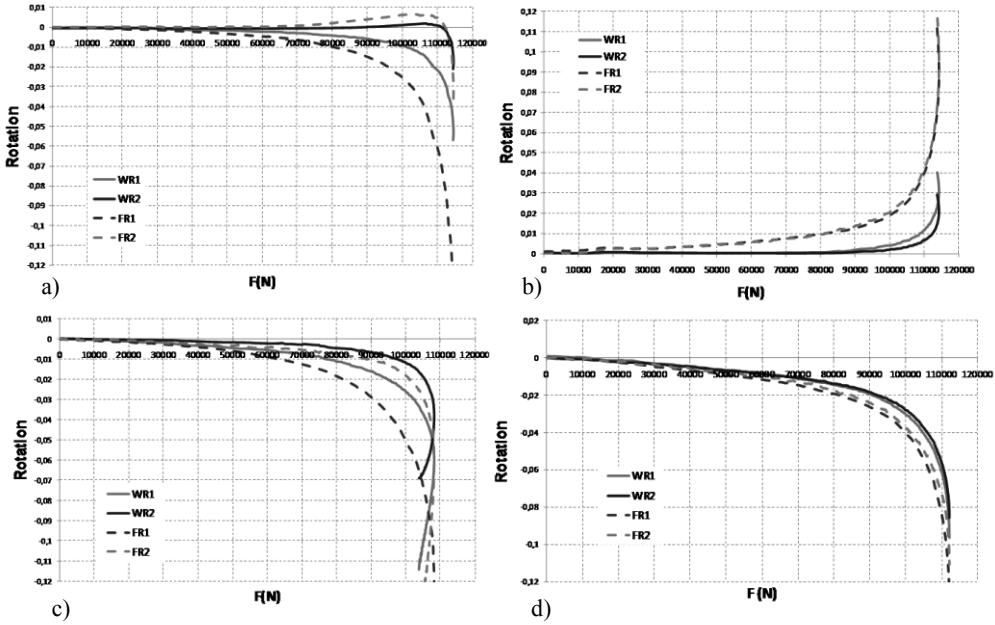

Figure 6: Measured rotations: a) S4-1200-3 Welded; b) S4-1200-2 Grips; c) S4-1200-1 Welded; d) S1-1650-2 Welded.

In order to quantify in some way the participation of each mode, the measured cross-section deformations were compared to GBT individual modes of deformation. This comparison was carried out applying a somewhat involved procedure that is not fully explained herein due to space reasons. The main idea of the procedure is that the corner displacement (ux,uy) and the rotations shown in figure 5a are applied to a beam finite element model of the cross-section, figure 5b. All the unknown nodal displacements of the cross-section are then deduced from the analyses of the beam model and, afterwards, a sort of simplified GBT modal identification procedure is applied [8]. The results can only be considered

approximations to the actual mode participation factors due to the important simplifications applied in the procedure. For instance, only transverse node displacements are taken into account, only linear GBT deformational modes are considered [9], the GBT deformational modes are calculated applying the equivalent thickness (1), and the corner displacement and rotations shown in figure 5a are derived considering that some parts of the cross-section underwent rigid rotations. However, in spite of all these simplifications, the results are rather reasonable.

Figure 7 presents the participation factors corresponding to the four graphs shown in figure 6. It should be pointed out that for the cross-sections analyzed in this investigation, the procedure tends to overestimate the participation of the global buckling modes.

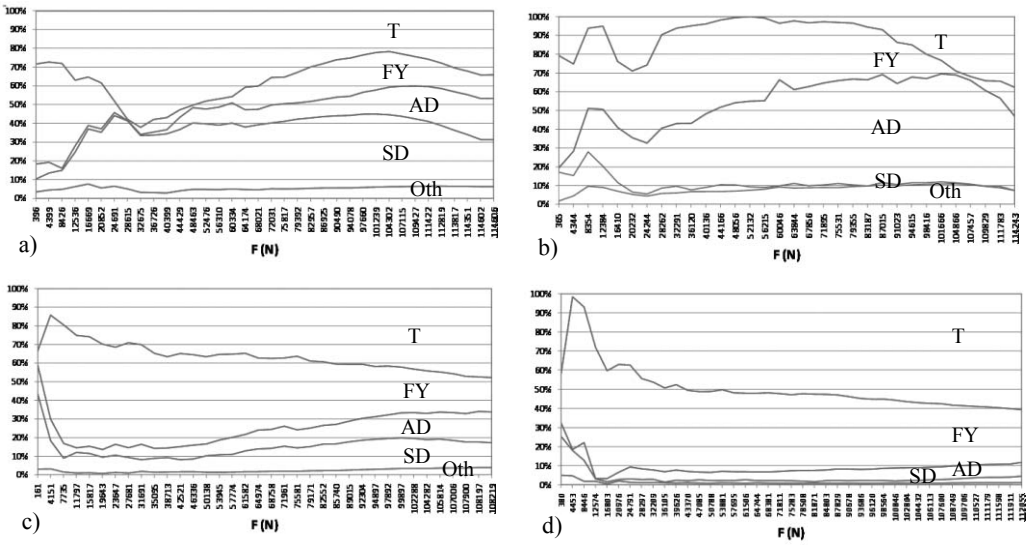

Figure 7: Participation factors: a) S4-1200-3 Welded; b) S4-1200-2 Grips; c) S4-1200-1 Welded; d) S1-1650-2 Welded.

5 DISCUSSION

Tables 2 and 3, and figures 6 and 7 show that the participation of the torsional (T) and flexural (FY) modes was significant in all tests; and that no dominant SD failure mode was observed. It seems that shorter members will have to be tested to capture this mode of buckling. These experimental results were in some way predicted by the FEM linear buckling analyses, since at the end of the critical SD mode interval, the distortional elastic buckling loads are almost equal to the global elastic buckling loads. As a consequence, any of these buckling modes can occur (see figure 3b).

It should be noticed that the curve of the global buckling loads derived from the linear buckling analyses (dashed curve in figure 3b), is a curve that corresponds to a combination of different modes. For short members (for example, about 600 mm for S4 cross-section), this curve is mainly AD dominant. As the member length increases, the AD mode progressively changes to a TF mode. Finally, for long members (for example, about 1800 mm for S4), the dominant mode is global buckling. Therefore, there is an interval of lengths were AD and TF coexist. In the present investigation, this mode combination has been experimentally observed and measured by means of the displacement transducers. It is verified that different combinations among distortional and global modes are relevant: AD + T + FY (figures 6b and 7b) or even SD + AD + T + FY (see figure 6a, 6c, 7a and 7c).

Neither the failure mode nor the ultimate load could be correctly predicted from the DSM calculations. These poor results are attributed to the use of equivalent thickness equation (1). Other approaches to determining an equivalent thickness in DSM calculations are being studied at the present time. A DSM approach using different equivalent thicknesses is being developed.

Finally, it is pointed out that members tested with special grips and members tested with welded load plates showed similar failure load and behavior.

6 CONCLUSIONS

The present investigation on the test method for distortional buckling of pallet rack uprights shows that rather short members, shorter than two times the critical distortional length, should be tested to capture a dominant distortional buckling mode. In the near future, additional tests will be carried out by the authors to verify this, and to investigate the effect of the distortional fixed end supports used in the experimental tests. Results of tests on single uprights will be compared to the results of tests on full upright frames (figure 1).

It is also observed that the effects of distortional buckling do not finish at the end of the symmetric distortional interval. There is an interval of longer lengths where the anti-symmetric distortional mode is combined with the torsional-flexural buckling mode. Further research is needed to know whether this combination should be considered in design.

Finally, it is pointed out that FEM linear analysis, carried out taking into account both perforations and the actual boundary conditions of the tests, demonstrated to be a useful tool to predict the behavior of the members tested in the present investigation. This analysis may not be very accurate when different modes have similar elastic buckling loads, but it gives an idea where to begin testing. In the future, it should also be investigated whether this analysis can be performed in CUFSM or GBTUL to make easier the determination of the specimen lengths.

REFERENCES

[1] EN 15512. Steel static storage systems – Adjustable pallet racking systems – Principles for structural design. European Standard. European Commitee for Standardization. March 2009.

[2] MH16.1:2008. Specification for the Design, Testing and Utilization of Industrial Steel Storage Racks. Rack Manufacturers Institute. 2008.

[3] AISI S910-08. Testing Method for Distortional Buckling of Cold-Formed Steel Hat Shaped Compressed Members. AISI Cold-Formed Design Manual. American Iron and Steel Institute. 2008.

[4] Silvestre, N. and Camotim, D., "Distortional buckling formulae for cold-formed steel C- and Z-section members. PartII-Validation and application", *Thin-Walled Structures*, 42, 1599-1629, 2004.

[5] Schafer, B.W. and Ádány S., "Buckling analysis of cold-formed steel members using CUFSM: conventional and constrained finite strip methods", *Eighteenth International Specialty Conference on Cold-formed Steel Structures*, Orlando, 2006.

[6] Bebiano, R., Pina, P., Silvestre, N., Camotim, D., GBTUL-Buckling and Vibration Analysis of Thin-Walled Members. DECivil/IST, Technical University of Lisbon, 2008.

[7] Davies, J.M., Leach, P. and Taylor, A., "The Design of Perforated Cold-Formed Steel Sections Subject to Axial Load and Bending", *Thin Walled Structures*, 29(1-4), 141-157, 1997.

[8] Ádány, S., Joó, A.L., Schafer, B.W., "Identification of FEM buckling modes of thin-walled columns by using cFSM base functions", *Proceedings of CIMS 2008 Fifth International conference on Coupled Instabilities in Metal Structures*, K.J.R. Rasmussen and T. Wilkinson (eds.), The University of Sydney, Sydney, 265-272, 2008.

[9] Silvestre, N. and Camotim, D., "Nonlinear Generalized Beam Theory for Cold-Formed Steel Members", *International Journal of Structural Stability and Dynamics*, 3(4), 461-490, 2003.

SDSS'Rio 2010 STABILITY AND DUCTILITY OF STEEL STRUCTURES
E. Batista, P. Vellasco, L. de Lima (Eds.)
Rio de Janeiro, Brazil, September 8 - 10, 2010

BEHAVIOUR OF EXPANDED METAL PANELS UNDER SHEAR LOADING

Phung Ngoc Dung[1], André Plumier[2]

[1]Department of Construction – Hanoi Architectural University – Viet Nam
e-mails: Dung.PhungNgoc@student.ulg.ac.be

[2]Department of Structural Engineering, University of Liege – 1, Chemin des Chevreuils, B-4000 Liège
e-mail: A.Plumier@ulg.ac.be

Keywords: Expanded Metal, Cyclic behaviour, Cyclic Tests, Hysterical Loops.

Abstract. *Experimental and theoretical study of expanded metal panels (EMP) has shown that they are useful for seismically retrofitting reinforced concrete moment resisting frames (RC-MRF). Although this product has merit of strength and ductility, it is at present only used for non-structural applications. There is no guidance existing to help the engineers determine the mechanical properties or to indicate in which field of the structures this product can be used. With the aims at providing quantitative data for these purposes and at introducing a simplified model of EMP working in shear, description and comparison of the results of 22 monotonic and cyclic experiments of 4 profiles of EMP in small and large scale is presented. Numerical approach with FINELG, a nonlinear finite element code developed at University of Liege, is used to calibrate and simulate the tests. A good correlation between tests and numerical simulations is observed.*

1 INTRODUCTION AND REVIEW OF PREVIOUS RESEARCH

EMP is a truss made from metal sheet by cuttings, cold-stretching and flattening [1]. Cuttings and cold-stretching make a metal sheet become a three-dimension structure. It becomes a two-dimension sheet by flattening. An expanded metal (EM) sheet – Figure 1 – has many rhomb-shape stitches, each with four bars having the same dimensions. It is characterized by four dimensions – LD, CD (the diagonals), A (the width), and B (the thickness of the bars). These dimensions are illustrated in Figure 2.

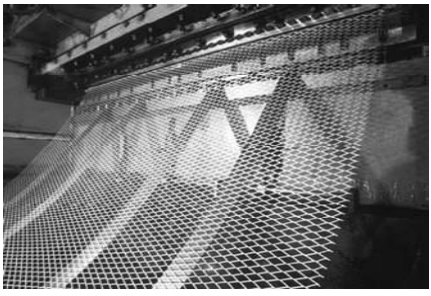

Figure 1 – Fabrication of expanded metal sheets

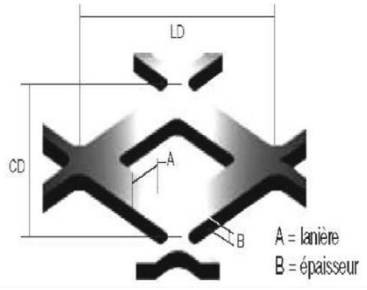

Figure 2 – An expanded metal rhomb-shape stitch

There are two types of the EM product: normal (or standard) and flattened types. In the normal type, rhomb-shape stitches are connected together with overlaps at the end of each bar. In contrast, there is no overlap between stitches in flattened type. They are continuously connected together to form a completely flattened sheet. At the moment, EM is mainly used for filters, in electrical applications or for the